Lactic Acid Extraction and Mass Transfer Characteristics in Slug Flow Capillary Microreactors

Susanti; Winkelman, Jozef G. M.; Schuur, Boelo; Heeres, Hero J.; Yue, Jun

Published in:
Industrial & Engineering Chemistry Research

DOI:
10.1021/acs.iecr.5b04917

Publication date:
2016

I&EC research
Industrial & Engineering Chemistry Research

Article

pubs.acs.org/IECR

Lactic Acid Extraction and Mass Transfer Characteristics in Slug Flow Capillary Microreactors

Susanti,[†] Jozef G. M. Winkelman,[†] Boelo Schuur,[‡] Hero J. Heeres,[†] and Jun Yue*[,†]

[†]Department of Chemical Engineering, University of Groningen, 9747 AG Groningen, The Netherlands
[‡]Faculty of Science and Technology, University of Twente, 7522 LW Enschede, The Netherlands

Supporting Information

ABSTRACT: Capillary microreactors operated under the slug flow regime were investigated for the separation of lactic acid from the aqueous phase using liquid−liquid reactive extraction. The experiments were performed at a 1:1 flow ratio of the aqueous to organic phases in a setup consisting of an inlet Y-type mixer connected with a poly(tetrafluoroethylene) capillary microreactor and subsequently an outlet Y-shape phase splitter. The extraction of lactic acid (intake: 0.11 and 0.055 M in water) using 15% (v/v) tri-*n*-octylamine in *n*-octanol under ambient conditions approached equilibrium after about 90 s in microreactors without noticeable emulsion formation. The measured reactive extraction performance in microreactors can be well described by a physical mass transfer model according to the penetration theory (developed from a model experimental study for the extraction of acetanilide from water to *n*-octanol) combined with an instantaneous irreversible reaction assumption.

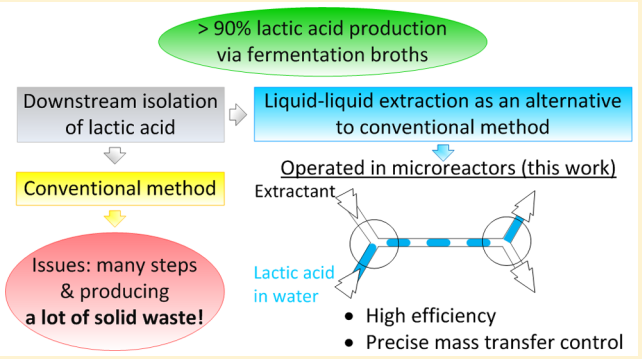

1. INTRODUCTION

In the past a few decades, the development of microreactors in the field of chemical and process engineering has received much research attention.[1−3] Microreactors offer good control over process parameters because of, among others, their well-defined flow pattern, efficient heat and mass transfer, and fast response and thus can be used to address case-specific drawbacks in conventional reactors such as transport limitations (in heat or mass transfer) leading to low yields, high waste generation, and cost issues related to the heavy use of solvents.[2−5] Advantages such as precise flow manipulation, good temperature control, enhanced safety, and vast possibilities for inline measurements make microreactors attractive tools not only for chemistry and catalyst investigation on the laboratory scale but also for chemical production on a pilot or industrial scale.[6]

Liquid−liquid extraction, involving mass transport (in the case of physical extraction) and reaction (in the case of reactive extraction) between two immiscible liquids, is an important separation technique widely used in analytical chemistry, biology, and chemical engineering. The extraction efficiency can be enhanced by maximizing the interfacial area (e.g., forming smaller droplets of the dispersed phase) and/or decreasing the mass transfer resistance. The use of microreactors for liquid−liquid extraction has been shown as a promising alternative to their macroscale counterparts.[7−13] This is mainly due to the significantly enhanced extraction efficiency therein because small characteristic dimensions in microreactors on the micrometer scale directly translate into a high surface to volume ratio (i.e., high interfacial area available for extraction) and a low mass transfer resistance.

Up to now, many reports have been published about the exploration of microreactors for liquid−liquid extraction involving experimental and modeling studies of the process.[12,13] Extraction operation, including the contact of two immiscible liquids and mixing and separation of both phases, has been successfully demonstrated in different geometrical microreactors. Because surface forces are dominant over body forces in microreactors, phase separation by gravity is difficult to implement. For some microreactor designs, phase separation was made relatively easy to enable almost complete separation at the microreactor outlet by means of physical supports such as membrane, guide structure, and partitioned wall.[13] Moreover, phase separation based on the preferential wettability has also been explored.[8,13]

Two types of common flow patterns can result when dealing with extraction between immiscible liquid phases in microchannels: slug flow characterized by the alternating flow of segmented fragments of immiscible fluids; parallel flow characterized by the side-by-side flow of immiscible fluids.[13,14] In parallel flow, mass transfer is limited mainly by molecular diffusion given the laminar flow nature and undisturbed side-by-side flow configuration in microchannels, although a higher

Received: December 23, 2015
Revised: March 22, 2016
Accepted: April 7, 2016
Published: April 7, 2016

DOI: 10.1021/acs.iecr.5b04917
Ind. Eng. Chem. Res. 2016, 55, 4691−4702

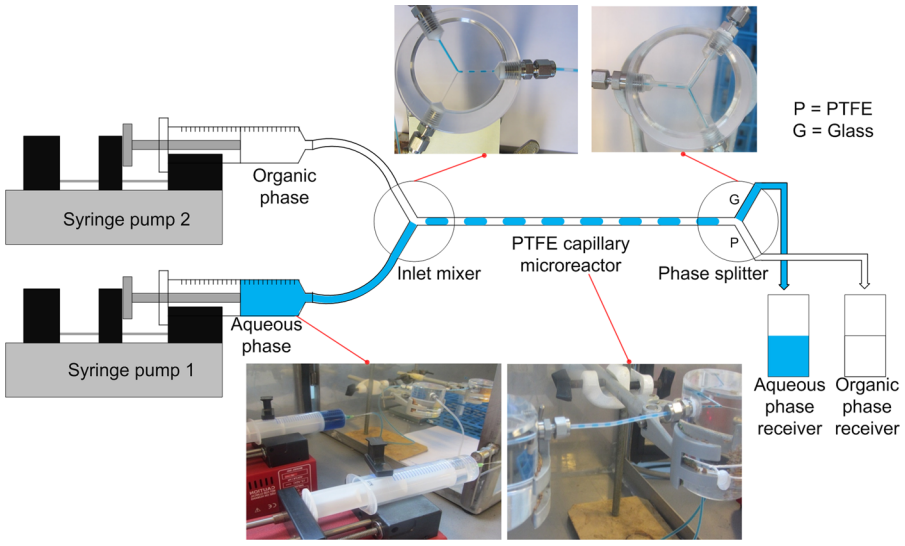

Figure 1. Schematic illustration of the experimental setup. Dye was applied in the aqueous phase for visualization purposes. In slug flow, the organic phase was the continuous phase, which preferentially wetted the PTFE microreactor wall, and the aqueous phase appeared as droplets.

mass transfer rate can be obtained for work at higher flow rates and/or in smaller microchannels.[15] A potential advantage in parallel-flow operation is that the separation between immiscible liquids at the microchannel outlet is relatively easy. Similar mass transfer performance between parallel and slug flows has been reported by Dessimoz et al.[14] for the (acid−base) neutralization reaction: the volumetric mass transfer coefficients in both flow patterns were obtained in a range of 0.2−0.5 s^{-1}. However, in contrast with parallel-flow operation, slug flow operation can obtain sufficiently higher interfacial area,[8] and mass transfer therein is significantly enhanced by the internal circulation inside each slug or droplet.[13,16]

Relatively fewer papers have been published about extraction under slug flow in microreactors compared with the case of parallel flow: some related to mass transfer study without reaction;[8,16−18] some involving reactive extraction.[11,14,19−21] Understanding mass transfer with reaction during extraction under slug flow in microreactors is not trivial given the somewhat complex nature of slug flow details. The published work so far is mostly concerned with empirical descriptions without physically sufficient reasoning. Therefore, an in-depth experimental and theoretical study of reactive extraction under slug flow in microreactors is necessary.

This work presents an experimental investigation into liquid−liquid reactive extraction in microreactors involving the extraction of lactic acid from the aqueous phase with tri-*n*-octylamine (TOA) as an extractant in *n*-octanol as the diluent. Lactic acid is an important biobased chemical used for the commercial production of poly(lactic acid) (a biobased and biodegradable plastic) and is currently produced by the fermentation of glucose or other six-carbon sugars (e.g., disaccharides like sucrose or lactose).[22−26] However, conventional lactic acid isolation from fermentation broths has some major drawbacks, for example, in the use of a large amount of alkali (i.e., lime) and relatively expensive sulfuric acid, the production of large amounts of solid waste (i.e., calcium sulfate), and the involvement of multistep purification.[23,27,28] Thus, liquid−liquid reactive extraction has been proposed as an attractive alternative to circumvent these issues for the isolation of lactic acid.[23]

Several developments are needed to bring lactic acid recovery by reactive extraction to an industrially competitive level. Interesting development has taken place in the selection and design of the extractants and diluents for lactic acid recovery recently.[29−34] Process intensification using microreactors could be applied under normal or especially extreme conditions (e.g., at elevated pressure and temperature) to explore more efficient extractive recovery regimes.[35,36] The traditional TOA in *n*-octanol system as tested in this work is suitable as a model solvent system for investigating fundamentals into mass transfer with chemical reaction in such reactive extraction. Moreover, amine extractants such as TOA have a promising performance for the separation of carboxylic acid from the aqueous phase.[24,37] Besides good capacity, high concentration of TOA exhibits low toxicity to *Lactobacillus delbrueckii* (i.e., one of the microorganisms in the fermentation process).[37] Therefore, reactive extraction using TOA in *n*-octanol combined with slug flow operation in microreactors is expected to hold great promise for developing an alternative technology for lactic acid isolation from fermentation broths.

In this work, the reactive extraction efficiency under slug flow operation in the capillary microreactors has been experimentally studied at different residence times. The influence of the residence time on mass transfer was studied by varying the total flow rate and/or length of the capillary microreactors. Two different lactic acid concentrations have been studied. The mass transfer behavior of the system has been well explained based on a simplified assumption of an irreversible instantaneous reaction regime prevailing in the organic phase, in combination with a physical mass transfer model developed according to the penetration theory from additional physical extraction experiments employing a model system for the extraction of acetanilide from water to *n*-octanol.

2. EXPERIMENTAL DETAILS

2.1. Material. Brilliant Blue FCF, Sudan III, acetanilide (≥99.5%), lactic acid (85%), and *n*-octanol (≥99%) were obtained from Sigma-Aldrich. Tri-*n*-octylamine (TOA) was obtained from Acros Organics. Two syringe pumps (model LA30, HLL Gmbh) were used for fluid delivery. Poly(tetrafluoroethylene) (PTFE) tubings (BOLA) were used as

DOI: 10.1021/acs.iecr.5b04917
Ind. Eng. Chem. Res. 2016, 55, 4691−4702

the capillary microreactors. The imaging system consisted of a digital camera (model Powershot SX220 HS, Canon).

2.2. Experimental Setup. A schematic experimental setup is shown in Figure 1. The aqueous and organic phases were delivered by two syringe pumps and introduced to a homemade 120°-angled Y-shape inlet mixer [1 mm inner diameter; made of poly(methyl methacrylate)] that was connected to a PTFE capillary microreactor of different lengths (1.6 mm outer diameter and 0.8 mm inner diameter). The two phases were separated at the end of the capillary microreactor using a homemade Y-shape splitter, which consisted of a PTFE tube and a glass tube of the same dimensions (i.e., 1.6 mm outer diameter and 0.8 mm inner diameter) that were inserted into the splitter block. The separation in the splitter was based on the preferential wettability difference: the aqueous phase has a strong affinity toward glass, whereas the organic phase has affinity toward PTFE. The samples from the two outlets of the splitter were collected in different vessels and analyzed.

2.3. Experimental Procedure. To investigate the liquid–liquid extraction and mass transfer characteristics in the microreactors, both physical and reactive extraction experiments were performed under ambient conditions (ca. 0.1 MPa and 25 °C). The physical properties of the solvents used are given in Table 1, as found from the literature.[38]

Table 1. Physical Properties of the Solvents Used (T = 25 °C)

liquid	density [kg/m^3]	viscosity [Pa s]	surface tension with water [N/m]
water	998	1×10^{-3}	
n-octanol	822	7.3×10^{-3}	8.19×10^{-3}

The partition coefficient and diffusivity of chemicals used in both phases are shown in Table 2. The partition coefficient (m) was determined from our experimental measurements: the experiments were performed in small glass vials of 20 mL, where 5 mL of the aqueous phase (i.e., containing acetanilide or lactic acid at various concentrations) was mixed with 5 mL of *n*-octanol; the phases were stirred at 500 rpm for 18 h and then allowed to settle for 2 h; the aqueous phase was separated and analyzed (vide infra). Then, m could be calculated as

Table 2. Properties of Chemicals Used (T = 25 °C)

chemical	partition coefficient between water and *n*-octanol	diffusivity [m^2/s] in the aqueous phase	diffusivity [m^2/s] in the organic phase
acetanilide	14.2[a]	1.1×10^{-9} [c]	1.34×10^{-10} [e]
lactic acid	0.18[a] (0.17[b])	1.01×10^{-9} [d]	1.18×10^{-10} [e]
TOA			1.19×10^{-10} [f]

[a]Our experimental data, calculated by eq 1. [b]Literature data from ref 40. [c]Literature data from ref 41. [d]Literature data from ref 42. [e]Calculated by eq 2 with diffusivity in water as a reference. [f]Literature data from ref 43.

$$m = \frac{C_{org,eq}}{C_{aq,eq}} \tag{1}$$

where $C_{org,eq}$ and $C_{aq,eq}$ are the equilibrium concentrations of the solute (i.e., acetanilide or lactic acid) in the organic and aqueous phases when only physical extraction takes place, respectively. The diffusivity of chemicals (D) used in both phases is either obtained from the literature or based on an approximation according to the Stokes–Einstein equation:[39]

$$\frac{D\mu}{T} = \text{constant} \tag{2}$$

2.3.1. Physical Extraction. To characterize mass transfer without reaction in the capillary microreactors, physical extraction experiments were performed using the water/*n*-octanol system with acetanilide as the mass transfer component (with its initial aqueous concentration being 1.5 or 0.81 mM). Pure *n*-octanol was used as the organic phase at the microreactor inlet. Extraction was carried out at several capillary microreactor lengths and flow rates (i.e., at varying residence times), with the flow ratio of the aqueous to organic phases being kept constant at 1:1. For slug flow operation, the residence time (τ) is calculated by

$$\tau = \frac{V_c}{Q_{aq} + Q_{org}} = \frac{\frac{\pi}{4} d_c^{\,2} L_c}{Q_{aq} + Q_{org}} \tag{3}$$

where V_c, d_c, and L_c are the volume, inner diameter, and length of the capillary microreactor, respectively. Q_{aq} and Q_{org} are the flow rates of the aqueous and organic phases, respectively. The volumetric flow rate of each phase was varied between 2.5 and 12.5 mL/h.

2.3.2. Reactive Extraction. The characteristics of reactive extraction in the capillary microreactors were investigated for lactic acid extraction with TOA. Lactic acid dissolved in water as the aqueous phase was extracted by TOA in *n*-octanol as the organic phase. TOA [15% (v/v)] in *n*-octanol was used for two typical initial concentrations of lactic acid in the aqueous phase (i.e., 0.11 and 0.055 M) based on the optimum extraction efficiency observed from the equilibrium study in our batch experiments: the batch experiments were performed in small glass vials of 20 mL, where 5 mL of 0.11 M lactic acid in water was mixed with 5 mL of *n*-octanol containing various amounts of TOA [ranging from 5 to 40% (v/v)]; the two phases were stirred at 500 rpm for 18 h and then allowed to settle for 2 h; the aqueous phase was separated and analyzed (vide infra).

The influence of the residence time was investigated by following the same procedure as that used in the physical extraction study (i.e., by changing the microreactor length and flow rate of each phase between 2.5 and 12.5 mL/h; the aqueous-to-organic flow ratio was 1:1).

2.3.3. Slug Flow Pattern Visualization. The use of equal flow rate between the aqueous and organic phases through an inlet 120°-angled Y-shape inlet mixer generated a stable slug flow in the subsequent capillary microreactor. For the purpose of visualizing the slug flow pattern (e.g., to enable the slug and droplet size measurement), Brilliant Blue FCF dye was added to the aqueous phase in additional physical extraction experiments, and Sudan III dye was added to the organic phase in additional reactive extraction experiments (with the concentration of each dye being 0.3 mM), while the other operational conditions remained unchanged. Note that the extraction performance was evaluated in the respective experiments in the absence of dyes. The slug flow pattern visualization in the capillary microreactors was made by camera snapshots (model Powershot SX220 HS, Canon) and repeated at least twice to ensure good reproducibility.

2.3.4. Analytical Procedure. The concentration of the solute in the aqueous phase was analyzed by a TIDAS UV–vis

DOI: 10.1021/acs.iecr.5b04917
Ind. Eng. Chem. Res. 2016, 55, 4691–4702

spectrophotometer (type RS 422, J&M Analytische mess-and Regeltechnik GmBH) at λ = 250 and 210 nm for acetanilide and lactic acid, respectively. The concentration of acetanilide or lactic acid (in all forms) in the organic phase was calculated according to the mass balance. All data provided are the averages from multiple experiments that showed good reproducibility.

3. RESULTS AND DISCUSSION

3.1. Mass Transfer in Physical Extraction. The physical extraction behavior of the microreactor system under slug flow operation was studied using a model system, being the extraction of acetanilide from water to *n*-octanol. The extraction efficiency and overall physical volumetric mass transfer coefficient were evaluated.

The extraction efficiency (η), defined as the ratio between the amount of material transferred from one phase to the other and the maximum transferable amount, is determined for the current physical extraction system according to the following equation:

$$\eta = \frac{C_{aq,0} - C_{aq,1}}{C_{aq,0} - C_{aq,eq}} \times 100\% \tag{4}$$

where $C_{aq,0}$ and $C_{aq,1}$ are the concentrations of the solute (i.e., acetanilide in this case) in the aqueous phase at the microreactor inlet and outlet, respectively. $C_{aq,eq}$ represents the concentration of the solute in the aqueous phase when physical extraction reaches equilibrium.

The extraction efficiency for the extraction of acetanilide from its aqueous solution into *n*-octanol as a function of the residence time (τ) in the present 0.8-mm-diameter capillary microreactors is shown in Figure 2. The extraction efficiency

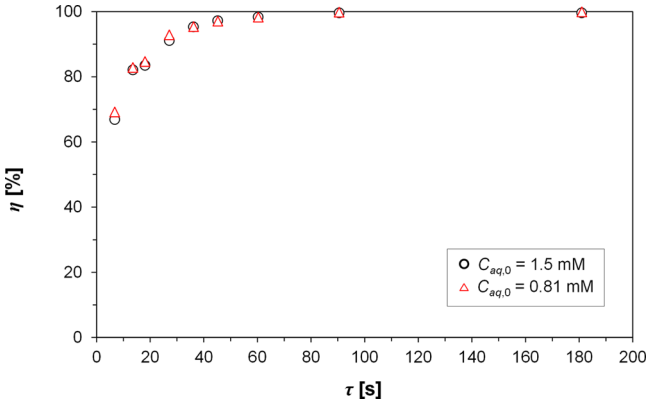

Figure 2. Extraction efficiency as a function of the residence time for physical extraction of acetanilide in 0.8-mm-diameter capillary microreactors. Varying residence time was achieved by changing the microreactor length and/or total flow rate (cf. eq 3).

increases with increasing residence time, approaching 100% after around 60 s. This indicates a fast extraction process primarily due to the enhanced physical mass transfer rates in the microreactor. At the same residence time, the use of different inlet concentrations of acetanilide in the aqueous phase (i.e., 1.5 and 0.81 mM) gave the same extraction efficiency. This implies that, under the investigated conditions, the extraction efficiency is independent of the inlet concentration of acetanilide and is only dependent on the residence time (see a detailed explanation in the Supporting Information, section A).

The overall physical volumetric mass transfer coefficient, $(K_{ov}a)_{Phys}$, is a characteristic parameter used to evaluate the performance of liquid−liquid extractors. With the inlet and outlet concentration values of acetanilide in both the aqueous and organic phases known, it is possible to calculate $(K_{ov}a)_{Phys}$ for the investigated microreactor system by conducting a mass balance. Then, it is obtained that

$$(K_{ov}a)_{Phys} = \frac{Q_{aq}(C_{aq,0} - C_{aq,1})}{V_c \Delta C_m} \tag{5}$$

where the mean concentration difference is defined as

$$\Delta C_m = \frac{\left(C_{aq,1} - \frac{C_{org,1}}{m}\right) - \left(C_{aq,0} - \frac{C_{org,0}}{m}\right)}{\ln\left(\frac{C_{aq,1} - \frac{C_{org,1}}{m}}{C_{aq,0} - \frac{C_{org,0}}{m}}\right)} \tag{6}$$

Here $C_{org,0}$ and $C_{org,1}$ are the concentrations of the solute (i.e., acetanilide) in the organic phase at the microreactor inlet and outlet, respectively. Because pure *n*-octanol was used at the inlet, $C_{org,0}$ = 0. Equation 5 represents an averaged calculation of $(K_{ov}a)_{Phys}$ in the present physical extraction experiments assuming plug-flow behavior and no radial concentration gradient in the bulk of each phase, which is commonly accepted for engineering calculations without the necessity of knowing the underlying hydrodynamics and mass transfer details.

Figure 3a shows the measured $(K_{ov}a)_{Phys}$ values in the capillary microreactors as a function of the microreactor length at different residence times. Here, the residence time was kept constant by varying the microreactor length and total flow rate (cf. eq 3). The $(K_{ov}a)_{Phys}$ value is higher at shorter residence times. Another important observation is that there is no difference in the measured $(K_{ov}a)_{Phys}$ values for the same residence time. This is further verified in Figure 3b, in which the measured $(K_{ov}a)_{Phys}$ values are plotted with variation in the phasic flow rate (with the aqueous-to-organic flow ratio being 1:1). For a given microreactor length, the $(K_{ov}a)_{Phys}$ value is higher at a higher total flow rate (i.e., at a shorter residence time). In other words, the variations in the total flow rate and microreactor length have no impact on $(K_{ov}a)_{Phys}$ as long as the residence time is the same. At a given phasic flow rate combination, the $(K_{ov}a)_{Phys}$ value along the capillary length is seen to decrease. This clearly suggests that the measured $(K_{ov}a)_{Phys}$ value is mainly a function of the residence time in the present experiments.

The measured $(K_{ov}a)_{Phys}$ value as a function of the residence time is further depicted in Figure 4, which is well described by the following relationship:

$$(K_{ov}a)_{Phys} = \frac{0.214}{\sqrt{\tau}} \tag{7}$$

Here, $(K_{ov}a)_{Phys}$ is in reciprocal seconds and τ in seconds. Because the aqueous-to-organic flow ratio was 1:1 in all of our experiments, the specific interfacial area (a) is practically the same for all operational conditions (as will be shown hereafter). Thus, it indicates that the overall physical mass transfer coefficient, $(K_{ov})_{Phys}$, is generally inversely proportional to $\sqrt{\tau}$, which is in agreement with Higbie's penetration theory.[44] In the present work, all of the measured $(K_{ov}a)_{Phys}$ values (in 0.8-

DOI: 10.1021/acs.iecr.5b04917
Ind. Eng. Chem. Res. 2016, 55, 4691−4702

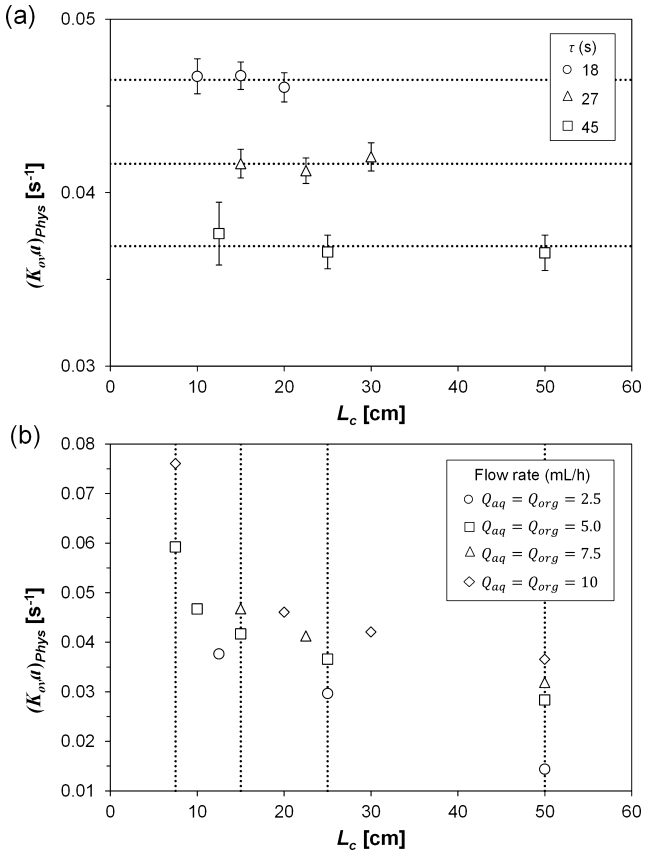

Figure 3. Measured overall physical volumetric mass transfer coefficient for physical extraction of 1.5 mM acetanilide in 0.8-mm-diameter capillary microreactors as a function of (a) the residence time and microreactor length and (b) the flow rate and microreactor length. The error bar in part a represents the standard deviation calculated from multiple measurements for a given condition.

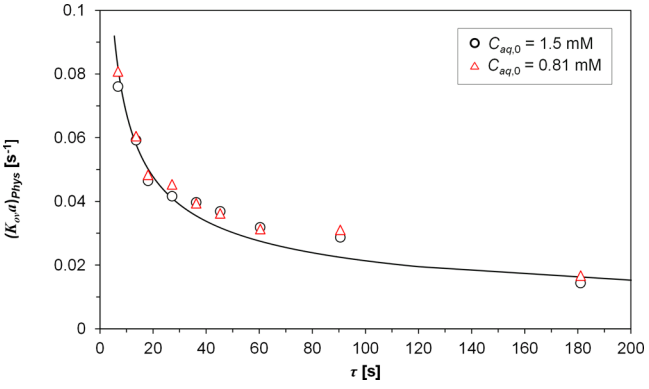

Figure 4. Overall physical volumetric mass transfer coefficient for physical extraction of acetanilide in 0.8-mm-diameter capillary microreactors. The solid line represents the fitting of the experimental data with eq 7.

mm-diameter capillary microreactors) are in the range of 0.01−0.09 s^{-1}, which are comparable to the values reported by Kashid et al.[8] (i.e., 0.02−0.32 s^{-1} for the extraction of succinic acid in the aqueous phase with *n*-butanol in the capillary microreactors having diameters of 0.75 and 1 mm). Figure 4 also shows that $(K_{ov}a)_{Phys}$ is independent of the inlet acetanilide concentration in the aqueous phase (i.e., 1.5 and 0.81 mM), which confirms the correctness of our experimental methods.

The agreement between the experimental measurements and Higbie's penetration theory as observed above has led us to formulate a simple model to describe the underlying mass transfer behavior during physical extraction in the investigated capillary microreactors. It is envisaged that the extraction of acetanilide from the aqueous phase to the organic phase under slug flow operation in the microreactor took place via the following mass transfer steps (Figure 5):[45,46] (1) transfer of

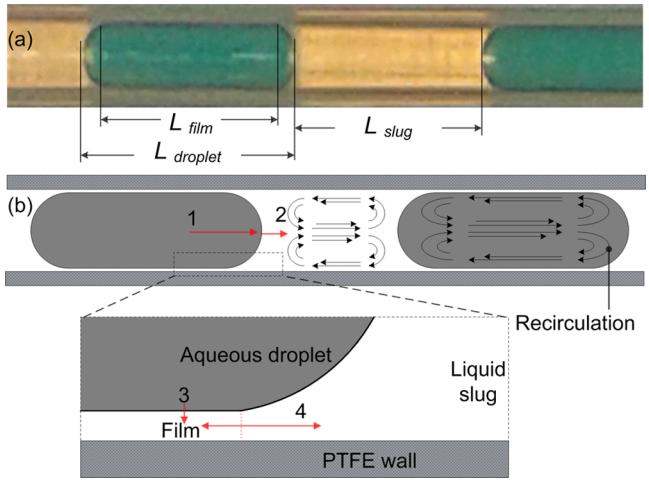

Figure 5. Mass transfer details in the capillary microreactor for physical extraction experiments: (a) Typical photograph of slug flow during physical extraction in the microreactor in which the organic phase was the continuous phase because of its good wetting on the PTFE wall and the aqueous phase appeared as droplets. Dye was applied in the aqueous phase for better visualization. (b) Schematic representation of mass transfer steps 1−4 in slug flow operation. The internal recirculation is viewed in a reference frame in which the microreactor wall moves from right to left at the droplet speed.

acetanilide from the bulk of the aqueous droplet (i.e., the droplet center) to the aqueous−organic interface; (2) transfer of acetanilide from the interface to the bulk of the organic slug (i.e., the slug center); (3) transfer of acetanilide from the interface to the organic film surrounding the aqueous droplet; (4) mixing of acetanilide between the organic film and the organic slug. Furthermore, mass transfer steps 1, 2, and 4 are facilitated by the internal recirculation in the droplet and liquid slug (cf. Figure 5b).[8,21,47]

In the present study, we simply assume that mass transfer steps 3 and 4 may be accounted for by a combination with mass transfer step 2. That is, no differentiation is made between the organic slug and the organic film. Thus, the entire interface will be used for mass transfer calculation in step 2. It is known that mass transfer into a quiescent liquid is described by Higbie's penetration theory at small Fourier numbers (typically <0.1).[48] If we neglect the internal recirculation in both the aqueous droplet and the organic slug, we can consider them both as stagnant fluids (i.e., in a reference frame with the microreactor wall moving at the droplet speed) and can thus define a characteristic Fourier number for each phase as

$$Fo_{org} = \frac{D_{org}\tau}{\left(\frac{L_{slug}}{2}\right)^2} \quad (8)$$

DOI: 10.1021/acs.iecr.5b04917
Ind. Eng. Chem. Res. 2016, 55, 4691−4702

$$Fo_{aq} = \frac{D_{aq}\tau}{\left(\frac{L_{droplet}}{2}\right)^2} \quad (9)$$

where D_{org} and D_{aq} denote the diffusivities of the solute (i.e., acetanilide in this case) in the organic and aqueous phases, respectively. For all physical extraction experiments, the calculated Fo_{org} ranges from 3.6×10^{-4} to 8.6×10^{-3} and Fo_{aq} from 2.3×10^{-3} to 4.9×10^{-2}. Given such small Fourier numbers, the local physical mass transfer coefficient in each phase (i.e., $k_{L,org}$ and $k_{L,aq}$) can be determined according to the penetration theory as[44,48]

$$k_{L,org} = 2\sqrt{\frac{D_{org}}{\pi\tau}} \quad (10)$$

$$k_{L,aq} = 2\sqrt{\frac{D_{aq}}{\pi\tau}} \quad (11)$$

Then, the overall physical mass transfer coefficient, $(K_{ov})_{Phys}$, is derived as

$$(K_{ov})_{Phys} = \frac{1}{\frac{1}{k_{L,aq}} + \frac{1}{mk_{L,org}}} \quad (12)$$

and thus the overall physical volumetric mass transfer coefficient is found as

$$(K_{ov}a)_{Phys} = \left(\frac{1}{\frac{1}{2\sqrt{\frac{D_{aq}}{\pi\tau}}} + \frac{1}{2m\sqrt{\frac{D_{org}}{\pi\tau}}}}\right)a \quad (13)$$

Here a represents the entire interfacial area available for mass transfer including the organic film region and slug region because the film contribution in mass transfer (i.e., mass transfer steps 3 and 4 as specified above) has been combined with the slug contribution. In the literature, it has been seen that considering the film region is important to determine the interfacial area in slug flow because the presence of the film gives a substantial rise in a for a long droplet,[47] and including the film gives much better agreement between the modeling study and the experimental results.[8]

With the presence of an organic film, the interfacial area is determined by

$$a = \frac{\pi d_{droplet}^{\ 2} + \pi d_{droplet} L_{film}}{\frac{1}{4}\pi d_c^{\ 2}(L_{droplet} + L_{slug})} \quad (14)$$

where $L_{droplet}$, L_{film}, and L_{slug} represent the lengths of the aqueous droplet, organic film, and organic slug, respectively (cf. Figure 5a). In this work, the measured droplet and slug lengths were found to be almost the same at all conditions with deviations of less than 5% (i.e., $L_{droplet} \approx L_{slug} \approx 4d_c$), which is reasonable because the current experiments were carried out at an aqueous-to-organic flow ratio at 1:1. In eq 14, $d_{droplet}$ is the diameter of the aqueous droplet end caps, which are approximated as hemispherical, and is assumed to be equal to the capillary microreactor diameter (i.e., $d_{droplet} \approx d_c$), based on the fact that the liquid film thickness is very thin under the present conditions given the low capillary numbers involved ($Ca = 2.4 \times 10^{-3}$–1.2×10^{-2}).[47,49] Here, Ca is the capillary number calculated as

$$Ca = \frac{\mu_{org}(j_{aq} + j_{org})}{\sigma} \quad (15)$$

where μ_{org} is the viscosity of the organic phase, j_{aq} and j_{org} are the superficial velocities of the aqueous and organic phases, respectively, and σ is the surface tension between the aqueous and organic phases. Furthermore, L_{film} can be calculated using the following relationship:

$$L_{film} = L_{droplet} - d_c \quad (16)$$

Under all of the present experimental conditions, the calculated interfacial area ranges from 2640 to 2730 m^2/m^3 (i.e., practically the same), which is comparable to the reported values for extraction of iodine with kerosene under slug flow operation in the capillary microreactors of similar diameters.[8]

Therefore, $(K_{ov}a)_{Phys}$ can be finally rearranged as

$$(K_{ov}a)_{Phys} = \left(\frac{1}{\frac{1}{2\sqrt{\frac{D_{aq}}{\pi\tau}}} + \frac{1}{2m\sqrt{\frac{D_{org}}{\pi\tau}}}}\right)\left[\frac{4L_{droplet}}{d_c(L_{droplet} + L_{slug})}\right] \quad (17)$$

The calculated $(K_{ov}a)_{Phys}$ value based on the developed model (i.e., eq 17) is compared with the measured $(K_{ov}a)_{Phys}$ value in Figure 6. The measured $(K_{ov}a)_{Phys}$ values are consistently about 2.6 times the model predictions. The underestimation in the model predictions can be explained primarily by the fact that not only does molecular diffusion contribute to mass transfer in slug flow but also the internal recirculation present in both the aqueous droplet and the organic slug enhances significantly interfacial mass transfer via convective diffusion (cf. Figure 5b).

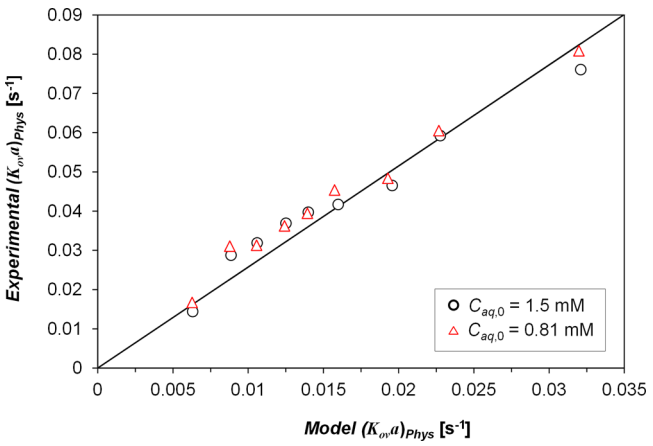

Figure 6. Comparison between the measured overall physical volumetric mass transfer coefficients for physical extraction of acetanilide in 0.8-mm-diameter capillary microreactors and model predictions with eq 17. The solid line represents the linear correlation with a slope of 2.6.

Then, the developed physical mass transfer model can be further refined as

$$(K_{ov}a)_{Phys} = 2.6\left(\frac{1}{\frac{1}{2\sqrt{\frac{D_{aq}}{\pi\tau}}} + \frac{1}{2m\sqrt{\frac{D_{org}}{\pi\tau}}}}\right)\left[\frac{4L_{droplet}}{d_c(L_{droplet} + L_{slug})}\right] \quad (18)$$

DOI: 10.1021/acs.iecr.5b04917
Ind. Eng. Chem. Res. 2016, 55, 4691−4702

A constant of 2.6 as found here suggests that the enhancement of internal recirculation in slug flow on an otherwise molecular diffusion-dominant mass transfer is not (or less) dependent on the phasic flow rate under the current experimental conditions at a 1:1 aqueous-to-organic flow ratio, which can be qualitatively analyzed by considering the concentration field inside the liquid slug and the droplet.

In the liquid slug, two counter-rotating vortices appear in a coordinate moving at the droplet speed, with closed streamlines and a pattern symmetrical about the center axis (cf. Figure 5b).[50,51] Within each vortex, convective transport of the solute takes place along the rotation direction while the dominant molecular transport is perpendicular to the rotation direction (described by the penetration theory given small Fourier numbers), affording the lowest solute concentration in the center region of each vortex (e.g., see Figure 3 in a recent simulation work by Zhang et al.[52] for a typical concentration field under liquid−liquid slug flow mass transfer in microreactors). If the recirculation is simply assumed to be extremely fast, one would imagine that the interfacial concentration is immediately built up at the outer boundary of each vortex (i.e., the circumference of the liquid slug and the center plane in a three-dimensional view, besides the interface at the slug end). Thus, the enhancement of internal recirculation in the liquid slug on mass transfer may be understood practically by the creation of an additional "fictitious interface area" available for mass transfer (i.e., the interfacial area of the liquid slug and that of the center plane). A similar analysis can be done for mass transfer enhancement in the droplet, where the additional "fictitious interface area" is the interfacial area of the liquid film and that of the center plane within the droplet (cf. Figure 5b).

In our experimental study, the liquid slug and droplet lengths were almost equal because of the 1:1 flow ratio employed. Then, the presence of internal recirculation in both the liquid slug and the droplet tends to yield an increase of $(K_{ov}a)_{Phys}$ by a factor of about 2 or slightly higher than 2 compared with the model prediction using eq 17 (i.e., the "fictitious interface area" is nearly the same for both the liquid slug and the droplet and is roughly equal to or slightly higher than a, as specified by eq 14 or as further elaborated in eq 17). The obtained constant of 2.6 in our experiments (cf. Figure 6) is in qualitative agreement with this estimation. On the basis of the above analysis, it is expected that the value of this constant may vary depending on the length ratio between the liquid slug and the droplet (or, equivalently, the aqueous-to-organic flow ratio).

However, it must be admitted that the above analysis is highly idealized and simplified without in-depth consideration of local slug flow hydrodynamics and mass transfer. A more elaborate analysis and fundamental insights into the enhancement of internal recirculation will be further sought in our ongoing numerical mass transfer study. The numerical work will allow one to reveal in great detail how the internal recirculation affects the concentration field and mass transfer rate and how the film contribution in mass transfer interacts precisely with the slug contribution.

With the refined mass transfer model (i.e., eq 18), the observed independence of the extraction efficiency on the inlet aqueous acetanilide concentration in the present experiments, as shown in Figure 2, can be well explained (see the Supporting Information, section A).

3.2. Mass Transfer in Reactive Extraction. Reactive extraction experiments involved the extraction of 0.11 or 0.055 M lactic acid from its aqueous phase with 15% (v/v) TOA (0.34 M) in *n*-octanol in the above-mentioned capillary microreactors. Lactic acid is a weak acid and dissociates in the aqueous phase according to

$$\mathrm{LA} \overset{K_a}{\rightleftharpoons} \mathrm{H^+} + \mathrm{LA^-} \tag{19}$$

where LA and LA^- represent the free and dissociated forms of lactic acid in the aqueous phase, respectively. The dissociation constant (K_a) is 1.38×10^{-4} at 25 °C.[53] The extent of lactic acid dissociation was found to be not very significant in our study: for concentration intakes of 0.11 and 0.055 M lactic acid, the average percentage of the dissociated form throughout the microreactor is below around 11% (see the Supporting Information, section B, for details). Thus, for a first approximation, we may neglect the dissociated form of lactic acid. The formation of complexes between lactic acid and TOA can be described by a simple additive model consisting of the following steps:[40]

$$[\mathrm{R_3N}] + \mathrm{LA} \overset{K_{11}}{\rightleftharpoons} [\mathrm{R_3N{\cdot}LA}] \tag{20a}$$

$$[\mathrm{R_3N{\cdot}LA}] + \mathrm{LA} \overset{K_{21}}{\rightleftharpoons} [\mathrm{R_3N{\cdot}(LA)_2}] \tag{20b}$$

$$[\mathrm{R_3N{\cdot}LA}] + [\mathrm{R_3N}] \overset{K_{12}}{\rightleftharpoons} [(\mathrm{R_3N})_2{\cdot}\mathrm{LA}] \tag{20c}$$

where R_3N and LA represent TOA and (free) lactic acid, respectively, with species in the organic phase marked with square brackets. K_{11}, K_{21}, and K_{12} are the equilibrium constants for the formation reaction of 1:1, 2:1, and 1:2 lactic acid−TOA complexes, respectively. Along with the formation of complexes, an equilibrium is also established between free lactic acid in both phases. In the current reactive extraction experiments, TOA was in excess, and thus the complexes were assumed to exist predominantly in the 1:1 form (cf. eq 20a), which is supported by the fact that K_{11} is much larger than K_{21} and K_{12} at the investigated conditions (see Table 2 in the work of Qin et al.[40]).

It is known that the isolation of lactic acid using liquid−liquid reactive extraction has a tendency to form emulsion, for example, in conventional reactors under high-shear turbulent mixing or in the hollow-fiber membrane extraction process.[23] In such cases, the generated droplet size can be well below 100 μm, leading to emulsion formation.[54] In our microreactors, there is an absence of turbulent mixing due to the laminar flow nature; thus, very small droplets could not be generated. Moreover, the droplets were expected to be generated at the Y-shape inlet mixer in the squeezing regime given low capillary numbers, where the forces involved in the droplet breakup process include the surface tension force, the shear force exerted by the continuous phase, and the force arising from pressure drop across the emerging droplet (which is the dominant force in the breakup dynamics).[55] The size of thus generated droplets was reproducible and several times the microreactor diameter under the investigated conditions (i.e., $L_{droplet} \approx 4d_c = 3.2$ mm). Hence, emulsions were not observed in the current capillary microreactors during the extraction of lactic acid with 15% (v/v) TOA in *n*-octanol. This ensures an easy separation of both the aqueous and organic phases based on the preferential wettability at the end of the capillary microreactors using the homemade Y-shape splitter (cf. Figure 1).

Reactive extraction in the current capillary microreactors was performed at different residence time values, and the

DOI: 10.1021/acs.iecr.5b04917
Ind. Eng. Chem. Res. 2016, 55, 4691−4702

corresponding extraction efficiency as a function of the residence time (τ) was plotted in Figure 7. Note that the

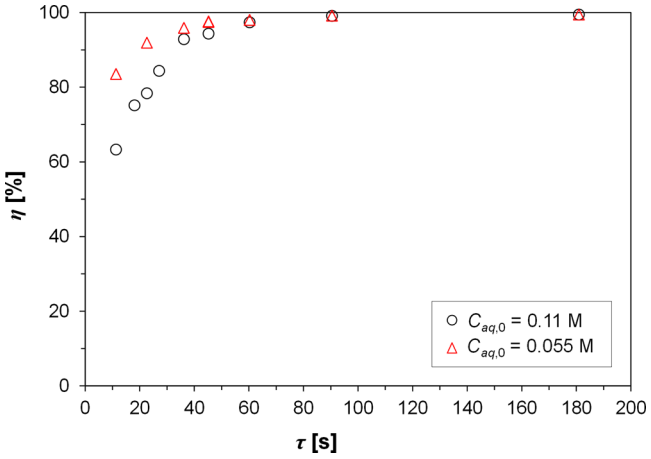

Figure 7. Extraction efficiency of lactic acid with 15% (v/v) TOA in *n*-octanol as a function of the residence time in 0.8-mm-diameter capillary microreactors.

extraction efficiency here was calculated using eq 4, in which $C_{aq,0}$ and $C_{aq,1}$ are the concentrations of the solute (i.e., lactic acid in this case) in the aqueous phase at the microreactor inlet and outlet, respectively, and $C_{aq,eq}$ represents the concentration of lactic acid in the aqueous phase when the reactive extraction reaches equilibrium, which was obtained from our additional experiments in batch reactors (see the Supporting Information, section C). Figure 7 reveals that, compared with the physical extraction case, the extraction efficiency in reactive extraction is dependent on not only the residence time but also the inlet lactic acid concentration in the aqueous phase. The lower the inlet lactic acid concentration, the higher the extraction efficiency. This trend is more obvious at short residence times at which the extraction is far from equilibrium. The observed dependence here is further explained in the Supporting Information, section C. The equilibrium seems to be approached at a residence time above 90 s in the investigated microreactors, which is considerably faster compared with our additional experiments in a small vial in batch mode (i.e., 5 mL organic phase was placed as a layer on the top of a 5 mL aqueous phase layer; TOA and lactic acid concentrations were kept unchanged; only the aqueous phase was stirred at a rate of 500 rpm in order not to distort the clear aqueous−organic interface). In this batch study, it took almost 1 h to reach equilibrium. Reactive extraction of several carboxylic acids using TOA at a high speed of the mixing rate was demonstrated by Rasrendra et al.[56] It involved the continuous reactive extraction in a centrifugal contactor separator, a device basically consisting of a rotating centrifuge in a static housing that combines efficient mixing and fast separation of two immiscible liquids. At a rotation speed of 3000 rpm, the extraction reached equilibrium after 15 min.[56] These comparison suggests that mass transfer in microreactors is significantly enhanced along with a fast intrinsic complexation rate between lactic acid and TOA.

To explain the observed extraction performance, a mass balance analysis for the extracted lactic acid from the aqueous phase to the organic phase was first performed over an elementary volume of the capillary microreactor as follows:

$$-Q_{aq}\,dC_{aq} = (K_{ov}a)_{Chem}\left(C_{aq} - \frac{C_{org}}{m}\right)dV_c \quad (21)$$

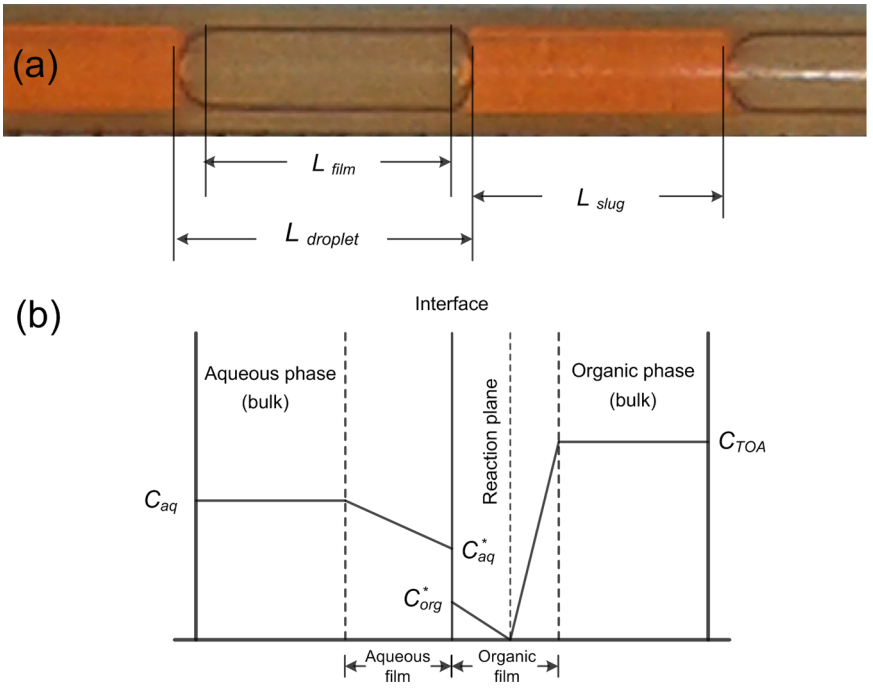

Figure 8. Mass transfer details in the capillary microreactor for reactive extraction experiments: (a) Typical photograph of slug flow during reactive extraction in the microreactor. Dye was applied in the organic phase for better visualization. (b) Schematically simplified representation of mass transfer with instantaneous reaction in slug flow according to the two-film theory. The film and bulk regions are for illustration purposes (not in scale).

DOI: 10.1021/acs.iecr.5b04917
Ind. Eng. Chem. Res. 2016, 55, 4691−4702

Here C_{aq} and C_{org} are the bulk concentrations (i.e., the average concentrations) of free lactic acid in the aqueous and organic phases, respectively. $(K_{ov}a)_{Chem}$ represents the overall chemical volumetric mass transfer coefficient in reactive extraction that further takes into account the enhancement of chemical reaction on the extraction rate.

Kinetics for lactic acid complexation with amine compounds in several diluents has been reported by Wasewar et al.[57] The reaction rate constant for the forward reaction of lactic acid with alamine-336 in *n*-octanol was found to be 24 s^{-1} (zero order in alamine-336; first order in lactic acid), and it is a relatively fast reaction. It has been known that alamine-336 is a mixture of straight-chain tertiary amines with 8−10 carbon atoms.[58] Therefore, TOA as a pure tertiary amine with eight carbon atoms, for a first approximation, is assumed to react with lactic acid in *n*-octanol instantaneously in the current microreactors under the investigated experimental conditions although the exact kinetic data for this system are not available yet. As such, this approximation neglects the reversible nature of the complexation (cf. eq 20), which is based on the fact that the equilibrium, if approached, only took place toward the outlet of the present microreactors (viz. extraction in a large portion of the microreactor was still far from equilibrium).

By assuming the presence of an irreversible instantaneous reaction regime, it is obtained that

$$C_{org} = 0 \tag{22}$$

This means that the free form of lactic acid is not present in the bulk of the organic phase. Equation 22 is also based on the fact that in our experiments TOA was never depleted at the microreactor outlet (i.e., the abundant TOA was assumed to bind any lactic acid transferred into the organic phase to predominantly form 1:1 complexes). If we represent the current reactive extraction in slug flow in a simplified view according to the two-film theory[59] (as shown in Figure 8a,b), mass transfer is assumed to take place inside a thin-film region in each phase adjacent to the interface. Inside the film region on the organic side, lactic acid meets with TOA at the reaction plane and reacts instantaneously there. In this simplified irreversible reaction model, as long as free TOA is available in the organic phase, free lactic acid does not exist in the bulk therein.

Then, eq 21 can be reduced to

$$-Q_{aq}\,dC_{aq} = (K_{ov}a)_{Chem}C_{aq}\,dV_c \tag{23}$$

Integration throughout the capillary microreactor leads to

$$(K_{ov}a)_{Chem} = \frac{Q_{aq}}{V_c}\ln\frac{C_{aq,0}}{C_{aq,1}} \tag{24}$$

Figure 9 shows the measured $(K_{ov}a)_{Chem}$ value according to eq 24 versus the residence time for reactive extraction of lactic acid at two different inlet concentrations in the microreactors (i.e., 0.11 and 0.055 M). A trend similar to that in physical extraction experiments was observed: the measured $(K_{ov}a)_{Chem}$ value increases with decreasing residence time and seems to be a function of the residence time regardless of the investigated flow rate or microreactor length. This implies the existence of a direct relationship between the overall volumetric mass transfer coefficients obtained from physical and reactive extraction experiments. However, unlike in the case of physical extraction, the measured $(K_{ov}a)_{Chem}$ value that takes into account the enhancement of chemical reaction depends on the inlet lactic acid concentration as well: the $(K_{ov}a)_{Chem}$ value is higher at lower inlet lactic acid concentration, which is more obvious at short residence times (e.g., <60 s); at long residence times, $(K_{ov}a)_{Chem}$ does not differ much for both inlet concentrations (see the Supporting Information, section D, for further explanations).

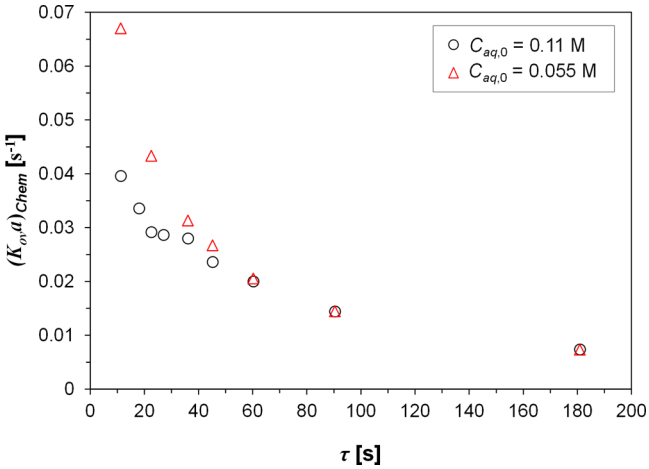

Figure 9. Overall chemical volumetric mass transfer coefficients as a function of the residence time measured in reactive extraction of lactic acid by 15% (v/v) TOA in *n*-octanol in 0.8-mm-diameter capillary microreactors.

From the investigated physical extraction experiments, it has been found that the overall physical volumetric mass transfer coefficient, $(K_{ov}a)_{Phys}$, is well represented by eq 18. Given the small Fourier numbers in the current reactive extraction experiments (Fo_{org} ranging from 5×10^{-4} to 6.8×10^{-3} and Fo_{aq} from 3.5×10^{-3} to 6×10^{-2}; calculated using eqs 8 and 9, in which D_{org} and D_{aq} denote the diffusivities of lactic acid in the organic and aqueous phases, respectively) and other similar flow conditions (i.e., the aqueous-to-organic flow ratio at 1:1), the criterion to derive eq 18 is also applicable here. Thus, according to the mass transfer scenario shown in Figure 8, it is reasonable to arrive at

$$(K_{ov}a)_{Chem} = 2.6\left(\frac{1}{\frac{1}{2\sqrt{\frac{D_{aq}}{\pi\tau}}} + \frac{1}{2mE_i\sqrt{\frac{D_{org}}{\pi\tau}}}}\right)\left[\frac{4L_{droplet}}{d_c(L_{droplet}+L_{slug})}\right] \tag{25}$$

where E_i is the instantaneous enhancement factor according to the two-film theory represented as[60]

$$E_i = 1 + \frac{D_{TOA}C_{TOA}}{zD_{org}C_{org}^*} \tag{26}$$

where C_{org}^* and C_{TOA} denote the interfacial concentration of free lactic acid and the bulk concentration of TOA on the organic phase side (cf. Figure 8b), respectively. z is the stoichiometric ratio between lactic acid and TOA, which is approximated as 1 here because of the assumption of the predominant formation of 1:1 complexes (cf. eq 20a). D_{TOA} is the diffusivity of TOA in the organic phase (*n*-octanol), which is almost equal to that of lactic acid (i.e., $D_{TOA} \approx D_{org}$; cf. Table 2). Hence, eq 26 can be further reduced to

DOI: 10.1021/acs.iecr.5b04917
Ind. Eng. Chem. Res. 2016, 55, 4691−4702

$$E_i = 1 + \frac{C_{TOA}}{mC_{aq}^*} \quad (27)$$

Here C_{aq}^* is the interfacial concentration of free lactic acid on the aqueous-phase side (cf. Figure 8b). Note that E_i in eq 27 should represent an average value in the microreactor for the estimation of $(K_{ov}a)_{Chem}$. Because C_{TOA} and C_{aq}* decreased as reactive extraction progressed along the microreactor, for a first approximation, we can simply take the average concentration between the microreactor inlet and outlet for the evaluation of E_i. That is

$$E_i \approx 1 + \frac{\frac{C_{TOA,0} + C_{TOA,1}}{2}}{m\left(\frac{C_{aq,0}^* + C_{aq,1}^*}{2}\right)} \quad (28)$$

where the subscripts 0 and 1 refer to the microreactor inlet and outlet, respectively. Because the interfacial concentrations (i.e., $C_{aq,0}$* and $C_{aq,1}$*) could not be directly measured from the experiments, E_i is further approximated based on the respective bulk concentrations of lactic acid in the aqueous phase (i.e., $C_{aq,0}$ and $C_{aq,1}$). Therefore,

$$E_i \approx 1 + \frac{\frac{C_{TOA,0} + C_{TOA,1}}{2}}{m\left(\frac{C_{aq,0} + C_{aq,1}}{2}\right)} \quad (29)$$

The predicted $(K_{ov}a)_{Chem}$ values using eqs 25 and 29 are compared with the experimental measurements for reactive extraction in Figure 10. A generally good agreement was

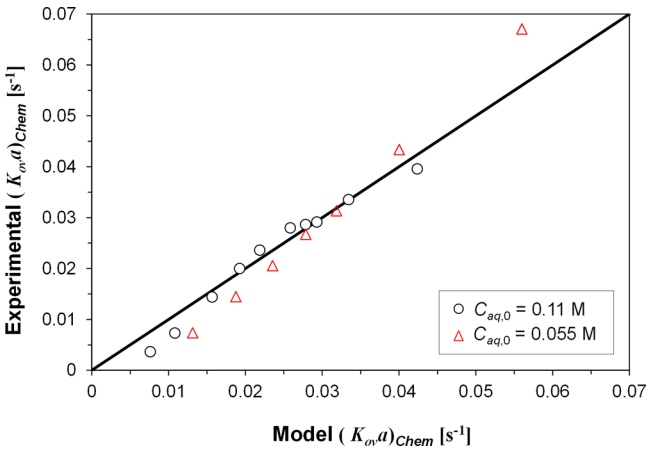

Figure 10. Overall chemical volumetric mass transfer coefficients based on the experiments versus the model predictions with eqs 25 and 29. The solid line represents the parity line. The operational conditions are the same as those described in Figure 9.

observed for both inlet concentrations of lactic acid, indicating that the measured reactive extraction performance is well described by the developed physical mass transfer model combined with the assumption of an irreversible instantaneous reaction regime. Because the bulk concentration of lactic acid in the aqueous phase (i.e., $C_{aq,0}$ and $C_{aq,1}$) was used for the approximation of E_i in eq 29 instead of the interfacial concentration (i.e., $C_{aq,0}$* and $C_{aq,1}$*), the actual E_i should be higher and thus the model using eqs 25 and 29 tends to underestimate the experimental measurements if the irreversible instantaneous reaction regime is warranted under the present conditions. However, the overall good agreement revealed in Figure 10 suggests that the complexation reaction rate might not always be fast enough to be considered as instantaneous compared with the physical mass transfer rate. In other words, the reaction regime could fall into an instantaneous one near the microreactor inlet and is likely to change into a fast or even slow reaction regime toward the microreactor outlet especially at long residence times at which the equilibrium tends to establish. This indicates a somewhat lower value of the actual enhancement factor than E_i calculated with eq 28 in the current experiments, as qualitatively considered in eq 29.

Two local trends seem to exist, as can observed in Figure 10: (1) at relatively low values of $(K_{ov}a)_{Chem}$ measured in the experiments, which correspond to long residence times, the developed model using eqs 25 and 29 seems to overestimate; (2) for 0.055 M lactic acid intake, such an overestimation seems more remarkable. Under such circumstances, the equilibrium could almost be approached at significant portions of the microreactor near the outlet. As a result, the reaction rate therein became significantly slow and the average value of the actual enhancement factor could be even lower than the approximation with eq 29, leading to the observed somewhat significant overestimation in the model predictions.

The overall good agreement between the measured $(K_{ov}a)_{Chem}$ values and model predictions using eqs 25 and 29 further indicates that the simple mass transfer model developed in physical extraction experiments (cf. eq 18) correctly depicts mass transfer characteristics in the current reactive extraction experiments given similar hydrodynamic conditions in both cases (i.e., slug flow operation, small Fourier numbers, and 1:1 aqueous-to-organic flow ratio). The assumption of an irreversible instantaneous reaction regime, although subject to further validation or improvement due to the lack of detailed kinetic data for complexation reaction between TOA and lactic acid in *n*-octanol and the reversible nature of the reaction, satisfactorily captures the interplay between mass transfer and reaction, as detailed in eqs 25 and 29. With the developed model, the observed dependence of the reactive extraction efficiency on the residence time and inlet concentration of lactic acid can be well explained (see the Supporting Information, section C).

4. CONCLUSIONS

Reactive extraction of lactic acid (0.11 or 0.055 M in water) using 15% (v/v) TOA in *n*-octanol was successfully performed under slug flow operation in 0.8-mm-diameter capillary microreactors, which was free from the tendency to form emulsion and therefore allowed the development of an alternative method for lactic acid isolation from fermentation broths with fewer operation steps. The extraction of lactic acid under the investigated microreactors approached equilibrium after around 90 s, which is considerably faster than our experiments in batch reactors and extraction of other carboxylic acid using TOA in centrifugal contactors.[56] The reactive extraction performance can be satisfactorily described by a simple mass transfer model according to the penetration theory (cf. eq 18) based on physical extraction experiments conducted in the same microreactor system for the extraction of acetanilide from water to *n*-octanol, combined with an irreversible instantaneous reaction assumption (cf. eqs 25 and 29).

The developed mass transfer model (eq 18) well describes our physical extraction results in the capillary microreactors

DOI: 10.1021/acs.iecr.5b04917
Ind. Eng. Chem. Res. 2016, 55, 4691−4702

under slug flow operation, with just one additional fitting parameter (i.e., 2.6 accounting for the enhancement of internal recirculation in slug flow on mass transfer). In combination with an irreversible instantaneous reaction assumption, the extended mass transfer model (cf. eqs 25 and 29) can describe the experimental measurements in $(K_{ov}a)_{Chem}$ for reactive extraction of lactic acid with good approximation. More fundamental insights into such an enhancement of the internal recirculation and the underlying reactive extraction characteristics will be made clear in our ongoing work including numerical simulation along with a detailed kinetic study for the complexation between TOA and lactic acid in *n*-octanol.

■ ASSOCIATED CONTENT

Supporting Information

The Supporting Information is available free of charge on the ACS Publications website at DOI: 10.1021/acs.iecr.5b04917.

Extraction efficiency as a function of the residence time in physical extraction, dissociation of lactic acid in the aqueous phase, and extraction efficiency and $(K_{ov}a)_{Chem}$ as a function of the residence time and inlet lactic acid concentration in reactive extraction (PDF)

■ AUTHOR INFORMATION

Corresponding Author

*Phone: +31 50 363 6522. E-mail: yue.jun@rug.nl.

Notes

The authors declare no competing financial interest.

■ ACKNOWLEDGMENTS

Financial support from the STW through Project 11404 (Chiral Separations by Kinetic Extractive Resolution in Microfluidic Devices) and input from all user committee members of the project are gratefully acknowledged.

■ NOMENCLATURE

a	interfacial area, m^2/m^3
C	concentration, mol/m^3
Ca	capillary number
D	diffusivity, m^2/s
d_c	inner diameter of the microreactor, m
Fo	Fourier number
j	superficial velocity, m/s
k_L	liquid-phase mass transfer coefficient, m/s
$K_{ov}a$	overall volumetric mass transfer coefficient, s^{-1}
L_c	length of the microreactor, m
m	partition coefficient
Q	flow rate, m^3/s
T	temperature, °C
V_c	volume of the microreactor, m^3

Greek Symbols

η	extraction efficiency, %
μ	dynamic viscosity, Pa s
σ	surface tension, N/m
τ	residence time, s

Subscripts

aq	aqueous phase
Chem	reactive extraction
eq	equilibrium
org	organic phase
Phys	physical extraction
TOA	tri-*n*-octylamine
0	inlet
1	outlet

■ REFERENCES

(1) McMullen, J. P.; Jensen, K. F. Integrated Microreactors for Reaction Automation: New Approaches to Reaction Development. *Annu. Rev. Anal. Chem.* **2010**, *3*, 19.

(2) Hessel, V.; Angeli, P.; Gavriilidis, A.; Löwe, H. Gas−Liquid and Gas−Liquid−Solid Microstructured Reactors: Contacting Principles and Applications. *Ind. Eng. Chem. Res.* **2005**, *44*, 9750.

(3) Elvira, K. S.; Solvas, X. C.; Wootton, R. C. R.; deMello, A. J. The Past, Present and Potential for Microfluidic Reactor Technology in Chemical Synthesis. *Nat. Chem.* **2013**, *5*, 905.

(4) Jähnisch, K.; Hessel, V.; Löwe, H.; Baerns, M. Chemistry in Microstructured Reactors. *Angew. Chem., Int. Ed.* **2004**, *43*, 406.

(5) Roberge, D. M.; Ducry, L.; Bieler, N.; Cretton, P.; Zimmermann, B. Microreactor Technology: A Revolution for the Fine Chemical and Pharmaceutical Industries? *Chem. Eng. Technol.* **2005**, *28*, 318.

(6) Yue, J.; Schouten, J. C.; Nijhuis, T. A. Integration of Microreactors with Spectroscopic Detection for Online Reaction Monitoring and Catalyst Characterization. *Ind. Eng. Chem. Res.* **2012**, *51*, 14583.

(7) Cai, Z.-X.; Fang, Q.; Chen, H.-W.; Fang, Z.-L. A Microfluidic Chip Based Liquid−liquid Extraction System with Microporous Membrane. *Anal. Chim. Acta* **2006**, *556*, 151.

(8) Kashid, M. N.; Harshe, Y. M.; Agar, D. W. Liquid-Liquid Slug Flow in a Capillary: An Alternative to Suspended Drop or Film Contactors. *Ind. Eng. Chem. Res.* **2007**, *46*, 8420.

(9) Kikutani, Y.; Mawatari, K.; Hibara, A.; Kitamori, T. Circulation Microchannel for Liquid−liquid Microextraction. *Microchim. Acta* **2009**, *164*, 241.

(10) Huh, Y. S.; Jeon, S. J.; Lee, E. Z.; Park, H. S.; Hong, W. H. Microfluidic Extraction Using Two Phase Laminar Flow for Chemical and Biological Applications. *Korean J. Chem. Eng.* **2011**, *28*, 633.

(11) Kamio, E.; Seike, Y.; Yoshizawa, H.; Matsuyama, H.; Ono, T. Microfluidic Extraction of Docosahexaenoic Acid Ethyl Ester: Comparison between Slug Flow and Emulsion. *Ind. Eng. Chem. Res.* **2011**, *50*, 6915.

(12) Ciceri, D.; Perera, J. M.; Stevens, G. W. The Use of Microfluidic Devices in Solvent Extraction. *J. Chem. Technol. Biotechnol.* **2014**, *89*, 771.

(13) Assmann, N.; Ładosz, A.; Rudolf von Rohr, P. Continuous Micro Liquid-Liquid Extraction. *Chem. Eng. Technol.* **2013**, *36*, 921.

(14) Dessimoz, A.-L.; Cavin, L.; Renken, A.; Kiwi-Minsker, L. Liquid−liquid Two-Phase Flow Patterns and Mass Transfer Characteristics in Rectangular Glass Microreactors. *Chem. Eng. Sci.* **2008**, *63*, 4035.

(15) Atencia, J.; Beebe, D. J. Controlled Microfluidic Interfaces. *Nature* **2005**, *437*, 648.

(16) Kashid, M. N.; Gupta, A.; Renken, A.; Kiwi-Minsker, L. Numbering-up and Mass Transfer Studies of Liquid−liquid Two-Phase Microstructured Reactors. *Chem. Eng. J.* **2010**, *158*, 233.

(17) Woitalka, A.; Kuhn, S.; Jensen, K. F. Scalability of Mass Transfer in Liquid−liquid Flow. *Chem. Eng. Sci.* **2014**, *116*, 1.

(18) Jovanović, J.; Rebrov, E. V.; Nijhuis, T. A.; Kreutzer, M. T.; Hessel, V.; Schouten, J. C. Liquid−Liquid Flow in a Capillary Microreactor: Hydrodynamic Flow Patterns and Extraction Performance. *Ind. Eng. Chem. Res.* **2012**, *51*, 1015.

(19) Burns, J. R.; Ramshaw, C. The Intensification of Rapid Reactions in Multiphase Systems Using Slug Flow in Capillaries. *Lab Chip* **2001**, *1*, 10.

(20) Burns, J. R.; Ramshaw, C. A Microreactor for the Nitration of Benzene and Toluene. *Chem. Eng. Commun.* **2002**, *189*, 1611.

(21) Jovanović, J.; Rebrov, E. V.; Nijhuis, T. A.; Hessel, V.; Schouten, J. C. Phase-Transfer Catalysis in Segmented Flow in a Microchannel: Fluidic Control of Selectivity and Productivity. *Ind. Eng. Chem. Res.* **2010**, *49*, 2681.

DOI: 10.1021/acs.iecr.5b04917
Ind. Eng. Chem. Res. 2016, 55, 4691−4702

(22) Vaidya, A. N.; Pandey, R. A.; Mudliar, S.; Kumar, M. S.; Chakrabarti, T.; Devotta, S. Production and Recovery of Lactic Acid for Polylactide—An Overview. *Crit. Rev. Environ. Sci. Technol.* **2005**, *35*, 429.
(23) Wasewar, K. L. Separation of Lactic Acid: Recent Advances. *Chem. Biochem. Eng. Q.* **2005**, *19*, 159.
(24) Wasewar, K. L.; Yawalkar, A. A.; Moulijn, J. A.; Pangarkar, V. G. Fermentation of Glucose to Lactic Acid Coupled with Reactive Extraction: A Review. *Ind. Eng. Chem. Res.* **2004**, *43*, 5969.
(25) Wasewar, K. L.; Heesink, A. B. M.; Versteeg, G. F.; Pangarkar, V. G. Equilibria and Kinetics for Reactive Extraction of Lactic Acid Using Alamine 336 in Decanol. *J. Chem. Technol. Biotechnol.* **2002**, *77*, 1068.
(26) Wee, Y.; Kim, J.; Ryu, H. Biotechnological Production of Lactic Acid and Its Recent Applications. *Food Technol. Biotechnol.* **2006**, *44*, 163.
(27) Taskila, S.; Ojamo, H. The Current Status and Future Expectations in Industrial Production of Lactic Acid by Lactic Acid Bacteria. In *Lactic Acid Bacteria—R&D for Food, Health and Livestock Purposes*; Kongo, J. M., Ed.; InTech: Rijeka, Croatia, 2013.
(28) Dusselier, M.; Van Wouwe, P.; Dewaele, A.; Makshina, E.; Sels, B. F. Lactic Acid as a Platform Chemical in the Biobased Economy: The Role of Chemocatalysis. *Energy Environ. Sci.* **2013**, *6*, 1415.
(29) Krzyżaniak, A.; Leeman, M.; Vossebeld, F.; Visser, T. J.; Schuur, B.; de Haan, A. B. Novel Extractants for the Recovery of Fermentation Derived Lactic Acid. *Sep. Purif. Technol.* **2013**, *111*, 82.
(30) Krzyzaniak, A.; Schuur, B.; de Haan, A. B. Equilibrium Studies on Lactic Acid Extraction with N,N-Didodecylpyridin-4-Amine (DDAP) Extractant. *Chem. Eng. Sci.* **2014**, *109*, 236.
(31) Marták, J.; Schlosser, Š. Extraction of Lactic Acid by Phosphonium Ionic Liquids. *Sep. Purif. Technol.* **2007**, *57*, 483.
(32) Marták, J.; Schlosser, Š.; Vlčková, S. Pertraction of Lactic Acid through Supported Liquid Membranes Containing Phosphonium Ionic Liquid. *J. Membr. Sci.* **2008**, *318*, 298.
(33) Oliveira, F. S.; Araújo, J. M. M.; Ferreira, R.; Rebelo, L. P. N.; Marrucho, I. M. Extraction of L-Lactic, L-Malic, and Succinic Acids Using Phosphonium-Based Ionic Liquids. *Sep. Purif. Technol.* **2012**, *85*, 137.
(34) Tonova, K.; Svinyarov, I.; Bogdanov, M. G. Hydrophobic 3-Alkyl-1-Methylimidazolium Saccharinates as Extractants for L-Lactic Acid Recovery. *Sep. Purif. Technol.* **2014**, *125*, 239.
(35) Blahušiak, M.; Schlosser, Š.; Cvengroš, J. Simulation of a New Regeneration Process of Solvents with Ionic Liquid by Short-Path Distillation. *Sep. Purif. Technol.* **2012**, *97*, 186.
(36) Blahušiak, M.; Schlosser, Š.; Marták, J. Simulation of a Hybrid Fermentation-Separation Process for Production of Butyric Acid. *Chem. Pap.* **2010**, *64*, 213.
(37) Choudhury, B.; Basha, A.; Swaminathan, T. Study of Lactic Acid Extraction with Higher Molecular Weight Aliphatic Amines. *J. Chem. Technol. Biotechnol.* **1998**, *72*, 111.
(38) Lide, D. R. *CRC Handbook of Chemistry and Physics: A Ready-Reference Book of Chemical and Physical Data*; CRC Press: Boca Raton, FL, 2007.
(39) Cussler, E. L. *Diffusion: Mass Transfer in Fluid Systems*; Cambridge University Press: New York, 1997.
(40) Qin, W.; Li, Z.; Dai, Y. Extraction of Monocarboxylic Acids with Trioctylamine: Equilibria and Correlation of Apparent Reactive Equilibrium Constant. *Ind. Eng. Chem. Res.* **2003**, *42*, 6196.
(41) Pradhan, A. A.; Heideger, W. J. On the Measurement of Liquid Phase Diffusivities for Slightly Soluble Solids. *Can. J. Chem. Eng.* **1971**, *49*, 10.
(42) Casalini, T.; Rossi, F.; Santoro, M.; Perale, G. Structural Characterization of Poly-L-Lactic Acid (PLLA) and Poly(glycolic acid) (PGA) Oligomers. *Int. J. Mol. Sci.* **2011**, *12*, 3857.
(43) Jeon, S.; Hong, W. H. Unsteady Mass Transfer Around Single Droplet Accompanied by Interfacial Extraction Reaction of Succinic Acid. *Hwahak Konghak* **2012**, *50*, 1021.
(44) Higbie, R. The Rate of Absorption of a Pure Gas into Still Liquid during Short Periods of Exposure. *Trans. AIChE* **1935**, *31*, 365.
(45) Yue, J.; Luo, L.; Gonthier, Y.; Chen, G.; Yuan, Q. An Experimental Study of Air−water Taylor Flow and Mass Transfer inside Square Microchannels. *Chem. Eng. Sci.* **2009**, *64*, 3697.
(46) Van Baten, J. M.; Krishna, R. CFD Simulations of Mass Transfer from Taylor Bubbles Rising in Circular Capillaries. *Chem. Eng. Sci.* **2004**, *59*, 2535.
(47) Ghaini, A.; Kashid, M. N.; Agar, D. W. Effective Interfacial Area for Mass Transfer in the Liquid−liquid Slug Flow Capillary Microreactors. *Chem. Eng. Process.* **2010**, *49*, 358.
(48) Yue, J.; Rebrov, E. V.; Schouten, J. C. Enhancement Factor for Gas Absorption in a Finite Liquid Layer. Part 1: Instantaneous Reaction in a Liquid in Plug Flow. *Chem. Eng. Technol.* **2012**, *35*, 679.
(49) Aussillous, P.; Quéré, D. Quick Deposition of a Fluid on the Wall of a Tube. *Phys. Fluids* **2000**, *12*, 2367.
(50) Kashid, M. N.; Gerlach, I.; Goetz, S.; Franzke, J.; Acker, J. F.; Platte, F.; Agar, D. W.; Turek, S. Internal Circulation within the Liquid Slugs of a Liquid−Liquid Slug-Flow Capillary Microreactor. *Ind. Eng. Chem. Res.* **2005**, *44*, 5003.
(51) Dore, V.; Tsaoulidis, D.; Angeli, P. Mixing Patterns in Water Plugs during Water/ionic Liquid Segmented Flow in Microchannels. *Chem. Eng. Sci.* **2012**, *80*, 334.
(52) Zhang, Y.; Zhang, X.; Xu, B.; Cai, W.; Wang, F. CFD Simulation of Mass Transfer Intensified by Chemical Reactions in Slug Flow Microchannels. *Can. J. Chem. Eng.* **2015**, *93*, 2307.
(53) Partanen, J. I.; Juusola, P. M.; Minkkinen, P. O. Determination of Stoichiometric Dissociation Constants of Lactic Acid in Aqueous Salt Solutions at 291.15 and at 298.15 K. *Fluid Phase Equilib.* **2003**, *204*, 245.
(54) Tadros, T. F. *Emulsion Formation and Stability*; Wiley-VCH Verlag GmbH & Co. KGaA: Weinheim, Germany, 2013.
(55) Garstecki, P.; Fuerstman, M. J.; Stone, H. A.; Whitesides, G. M. Formation of Droplets and Bubbles in a Microfluidic T-junction-Scaling and Mechanism of Break-up. *Lab Chip* **2006**, *6*, 437.
(56) Rasrendra, C. B.; Girisuta, B.; van de Bovenkamp, H. H.; Winkelman, J. G. M.; Leijenhorst, E. J.; Venderbosch, R. H.; Windt, M.; Meier, D.; Heeres, H. J. Recovery of Acetic Acid from an Aqueous Pyrolysis Oil Phase by Reactive Extraction Using Tri-N-Octylamine. *Chem. Eng. J.* **2011**, *176−177*, 244.
(57) Wasewar, K. L.; Pangarkar, V. G.; Heesink, A. B. M.; Versteeg, G. F. Intensification of Enzymatic Conversion of Glucose to Lactic Acid by Reactive Extraction. *Chem. Eng. Sci.* **2003**, *58*, 3385.
(58) Park, S.-J.; Kwon, R.-H.; Choi, Y.-Y. Solid−liquid Equilibrium and Mixture Properties for the Binary Systems of Alamine 336 with Decane, Dodecane, and 1-Dodecanol. *Fluid Phase Equilib.* **2014**, *361*, 130.
(59) Westerterp, K. R.; van Swaaij, W. P. M.; Beenackers, A. A. C. M. *Chemical Reactor Design and Operation*; Wiley: New York, 1988.
(60) Danckwerts, P. V. *Gas−Liquid Reactions*; McGraw-Hill: New York, 1970.

DOI: 10.1021/acs.iecr.5b04917
Ind. Eng. Chem. Res. 2016, 55, 4691−4702